Hindawi
International Journal of Electrochemistry
Volume 2019, Article ID 5743952, 11 pages
https://doi.org/10.1155/2019/5743952

Research Article

The Electrochemical Variation of a Kind of Protein Staining and Food Dye as a New Corrosion Inhibitor on Mild Steel in Acidic Medium

Demet Özkır

Niğde Ömer Halisdemir University, Department of Chemistry, Niğde 51200, Turkey

Correspondence should be addressed to Demet Özkır; dozkir@ohu.edu.tr

Received 8 December 2018; Accepted 17 January 2019; Published 3 March 2019

Academic Editor: Adalgisa Rodrigues de Andrade

In this study, the relevance of a food dye, namely, Fast Green-FCF (FG-FCF), was surveyed as a new inhibitor for mild steel in HCl solution. This effect was specified by electrochemical impedance spectroscopy (EIS), one of the most widely used measurement techniques. As a result of the increment of the inhibitor concentration, it was seen that the values of polarization resistance increased and covered the metal surface of FG-FCF like a blanket. Tests endorse that the FG-FCF is chemically adsorbed on mild steel surface, according to the Langmuir isotherm. With surface characteristic analyses, such as field emission scanning electron microscope (FESEM) and atomic force microscope (AFM), it was further determined that the metal surface in HCl of FG-FCF was protected. By applying the hydrogen gas evolution technique, FG-FCF has been proven to provide the lowest surface area with all inhibited solutions from the blank due to its strong adsorption to the metal surface. Finally, it has been clarified that FG-FCF can be practically used as a good corrosion inhibitor for mild steel with the supported results.

1. Introduction

Modification of chemicals in metals affects their properties, such as corrosion resistance and strength. Mild steel is very strong due to the low carbon content it contains. Strong in material science is a complex term. It has high resistance to rupture. Unlike higher carbon steels, soft steel is very soft even when it is cold. Higher carbon steels generally break or crack under stress, while it bends or distorts [1]. Mild steel is particularly admirable for construction due to its workability. It also has great economic importance and some advantages which are highly demanded by many industries. As the demand for its use increases, corrosion prevention occurs. Corrosion is an important phenomenon that needs to be prevented all over the world. In fact, the aging of human beings is one of the living and vital examples of corrosion. The economic and material losses it causes are extremely important for a country's income [2, 3]. The use of inhibitors to prevent metal corrosion in aggressive media like a hydrochloric acid is a highly preferred application. Corrosion inhibitors are categorized into inorganic and organic inhibitors. The use of the majority of inorganic inhibitors is generally avoided because of their heavy metal content, environmental risks, and biotoxic effects. On the contrary, it would be more appropriate to use nontoxic, effective, and healthy organic inhibitors than to use an inorganic inhibitor which has a toxic effect in preventing metal corrosion [4, 5]. Frequently, many organic compounds containing different types of heteroatoms are tapped to prevent the corrosion of mild steel, can form covalent bonds with metals, and then adsorb onto the metal surface [6–8]. According to the literature findings of many researchers, some heterocyclic organic compounds which contain nitrogen, sulphur, and oxygen in their molecular structure are active as corrosion inhibitors [9–14]. The inhibitors should be exceedingly influential even at very low concentrations. Dyes are among the most commonly used corrosion inhibitors [15, 16]. Dyes like Fast Green FCF can be adsorbed onto the metal surface and change the features of the metal, such as its prone to corrosion and adsorption characteristics. The corrosion preventing properties of such dyes are not focused on a uniform process. In other words, it depends primarily on the metal, the

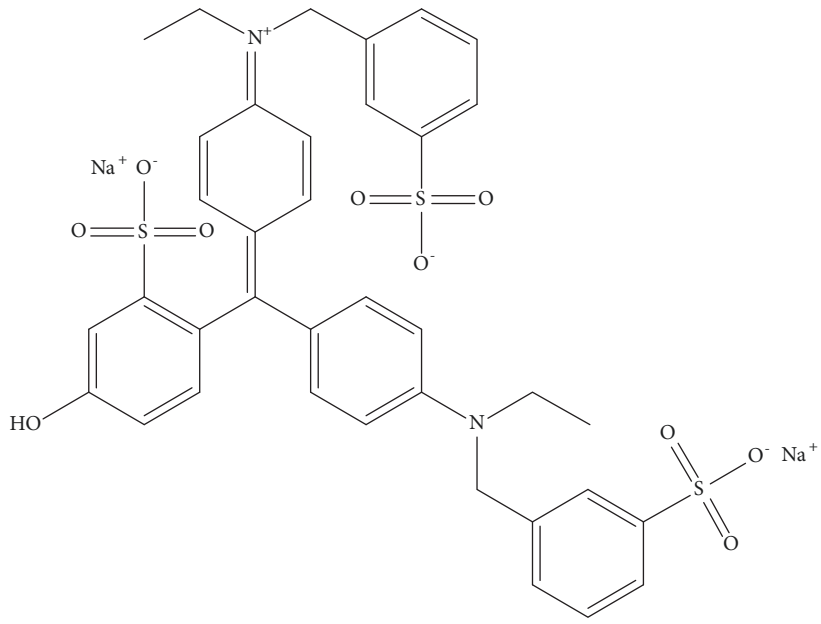

Figure 1: The molecular structure of Fast Green-FCF used as an inhibitor.

aggressive environment, the structure, and concentration of the organic inhibitor compound [11, 17]. Recently, Pareek and coworkers have found that a dye, namely, "4-amino-3-(phenyldiazenyl)benzo[4, 5]imidazo[1,2-a]pyrimidin-2(1H)-one", can be used as an inhibitor in inhibiting corrosion of copper in 3.5 wt.% (by weight) NaCl solution [18]. A study by Ebenso and Oguzie has revealed that some organic dyes, namely, safranine-o, thymol blue, and fluorescein-Na, are effective inhibitors for mild steel in sulphuric acid solution [19].

The Fast Green-FCF has a captivating effect due to its molecular structure and had remarkable properties before starting this study. Among the reasons for the preference of this dye as an inhibitor are the presence of nitrogen, oxygen, and sulphur atoms in their structure and their ability to act as an adsorption centre, as well as having a large and aromatic molecular structure. Some of the various dyes used in the industry cause considerable hazards [20, 21], while others are used in the food additive or the pharmaceutical and cosmetic industries [22–25]. Fast Green-FCF is also used in scientific research such as food dye and protein staining as well as electrophysiological experiments [26–29]. Up to now, there has been no literature describing the effects of Fast Green-FCF on the corrosion inhibition of mild steel in the 1.0 M HCl solution. From this point of view, in this study, it has been investigated whether Fast Green-FCF, which is used in both protein staining and food dye, can be corrosion inhibitor for mild steel in addition to the known usage areas.

2. Materials and Methods

One of the materials used in the experiments is mild steel electrode and its chemical composition is presented in Table 1.

All electrochemical tests were realized using CHI 660B electrochemical analyser with conventional three-electrode cell. The all specimens were emplaced in polyester and then degreased with acetone and washed and dried before the usage. The first electrode was the working electrode as mild steel and had a surface area which was 0.5024 cm^2. They were abraded with 150, 600, and 1000 grid emery papers before the immersion in test solutions. The connection was made with a copper wire for conductivity to the mild steel electrodes. The secondly, it was the counter electrode which had a surface area of 1 cm^2 as platinum. The third one was the reference electrode used as Ag/AgCl. All chemicals used in the experiments were purchased from Merck Chemical Company. The molecular structure of FG-FCF, which is the IUPAC name {2-((E)-(4-(ethyl(3-sulfonatobenzyl)amino)phenyl)((E)-4-(ethyl(3-sulfonatobenzyl)iminio)cyclohexa-2,5-dien-1-ylidene)methyl)-5-hydroxybenzene sulfonate}, is presented in Figure 1.

Table 1: The chemical composition of the mild steel electrodes.

Element	%	Element	%	Element	%
(C)	0.08400	**(Si)**	0.10200	**(Mn)**	0.40900
(P)	0.01100	**(S)**	0.01900	**(Cr)**	0.06030
(Mo)	0.01040	**(Ni)**	0.07890	**(Al)**	Trace
(Co)	0.00198	**(Cu)**	0.21700	**(Nb)**	0.00222
(Ti)	Trace	**(V)**	0.01100	**(W)**	Trace
(Pb)	Trace	**(Sn)**	0.01620	**(Sb)**	Trace
(Fe)	Remain				

1.0 M HCl solution was prepared by dilution of analytical grade 37% HCl with distilled water and this solution was used as a blank solution to compare the inhibitor efficiency. In addition, all inhibitor concentrations were studied between $1.0x10^{-5}$ M and $1.0x10^{-3}$ M. Before each electrochemical

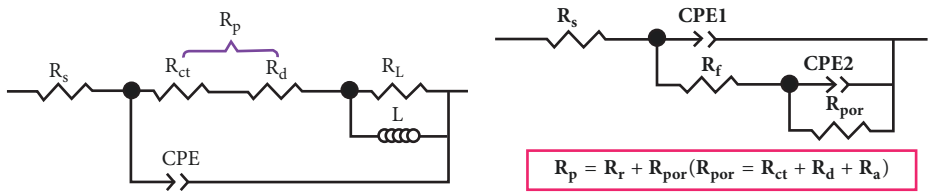

(a) Uninhibited solution (b) Inhibited solutions

Figure 2: Proposed equivalent circuit models for uninhibited and inhibited solutions (R_s: solution resistance, R_{ct}: charge transfer resistance, R_d: diffuse layer resistance, R_a: resistance of accumulated species at metal/solution interface, L: inductance, R_L: inductive resistance, R_f: film resistance, R_{por}: pore resistance, *CPE1*: film capacitance, and *CPE2*: double layer capacitance).

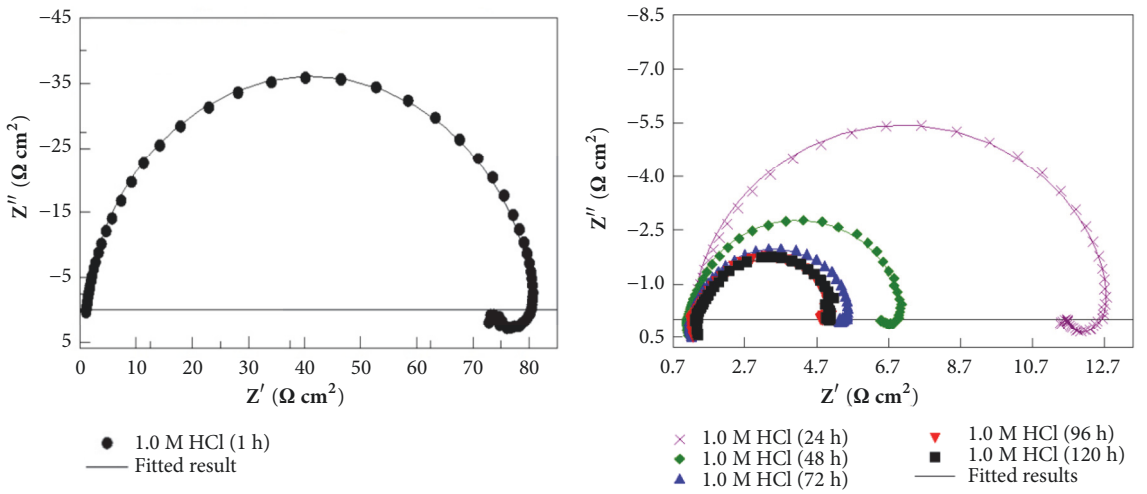

Figure 3: Nyquist plots obtained for different exposure times in uninhibited solutions.

experiment, the system was allowed to equilibrate for 1 hour and measurements were performed according to the determined open circuit corrosion potential (E_{corr}). EIS tests were realized in the frequency range of 10^5 to $5x10^3$ Hz with 5 mV amplitude. Firstly, the equivalent circuits of the system are created for EIS tests and all impedance plots were presented by fitting the Zview2 software program for data research. EIS experiments were also studied at ±0.250 V (Ag/AgCl) potential ranges from E_{corr} and polarization resistance (R_p) values were determined. R_p values were plotted against measured E_{corr} values and the maximum peak in this plot corresponds to potential of zero charge (E_{pzc}) [30, 31].

In order to examine how FG-FCF protects the mild steel surface in acidic solution in time, hydrogen evolution (V_{H2}-t) and EIS methods are applied during 1-120 h immersion times [31]. Mild steel specimens were immersed in a beaker 150 mL of inhibited and uninhibited solutions without stirring in order to analyse and compare the inhibition influence of the FG-FCF over a longer time. For the hydrogen evolution test, one-end closed and specially constructed burettes were used. The burettes were filled with all test solutions and inverted into the beakers containing the test solutions and the mild steel electrodes. It should be noted here that the mild steel electrode should be closed to the mouth of the filled burette.

Surface characteristics of mild steel electrodes were examined after 120 h of exposure time in 1.0 M HCl with and without FG-FCF inhibitor by the atomic force microscope (Veeco Multimode 8 Nanoscope 3D model) and high-resolution FESEM technique (ZEISS GEMINISEM 500 model) with computer controlled.

3. Results and Discussion

3.1. EIS and Immersion Time Measurements. EIS findings are usually commented in terms of electrical equivalent circuits that can be used to characterize the electrical properties of the interfaces.

In Figure 2, equivalent circuits used for both inhibitor and noninhibitor solutions of the system are given. The Nyquist plots of mild steel which were acquired in various concentrations of FG-FCP with and without 1.0 M HCl solution at 298 K after different immersion times were demonstrated in Figures 3 and 4.

When looking at the equivalent circuits proposed for both media, there are differences in the circuit elements of them. The biggest difference is inductive resistance (R_L) and inductance (L) originating from the inductive loop in

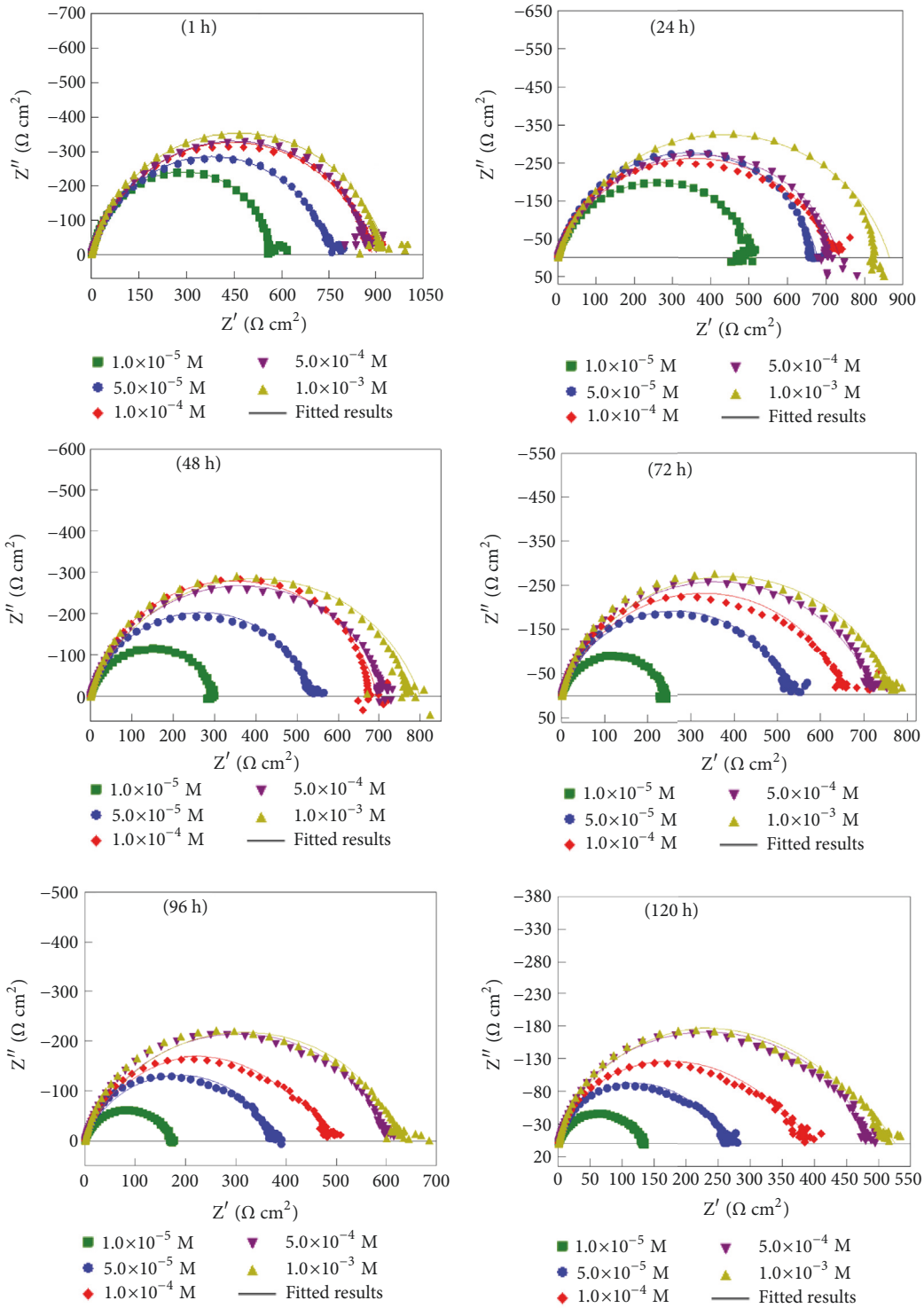

Figure 4: Nyquist plots obtained for different exposure times in inhibited solutions.

uninhibited solution. There are two *CPE* circuit elements in the inhibited solutions.

One of them is the double layer capacitance (CPE_{dl}) and the other is the film layer capacitance (CPE_{film}), which is responsible for the inhibitor film formed on the mild steel surface. The impedance parameters such as R_L, L, R_p, solution resistance (R_s), and constant phase element (*CPE*) obtained from Zview2 software program and the inhibition efficiency (η%) values calculated from polarization resistances are evaluated for each immersion time in Table 2.

Referring to the Nyquist diagrams in Figures 3 and 4, the depressed semicircle in the blank solution states that the

Table 2: The EIS parameters of mild steel specimens in inhibited and uninhibited solutions at different immersion times.

Time/C (M)	R_s (Ω cm^2)	R_p (Ω cm^2)	CPE (μF/cm^2)	n	R_L (Ω cm^2)	L (H)	η (%)
1 h							
Blank	1.2	72	110	0.94	8	4	-
$1.0x10^{-5}$	1.3	576	81	0.89	-	-	87.5
$5.0x10^{-5}$	1.4	755	75	0.87	-	-	90.4
$1.0x10^{-4}$	1.1	888	70	0.86	-	-	91.9
$5.0x10^{-4}$	1.1	902	62	0.82	-	-	92.0
$1.0x10^{-3}$	1.2	935	54	0.81	-	-	92.3
24 h							
Blank	1.2	11	2600	0.95	1.3	1.1	-
$1.0x10^{-5}$	1.1	520	1392	0.84	-	-	97.9
$5.0x10^{-5}$	1.3	676	862	0.83	-	-	98.4
$1.0x10^{-4}$	1.2	715	392	0.81	-	-	98.5
$5.0x10^{-4}$	1.2	735	197	0.80	-	-	98.5
$1.0x10^{-3}$	1.1	864	95	0.81	-	-	98.7
48 h							
Blank	1.1	5	10123	0.94	0.7	1	-
$1.0x10^{-5}$	1.1	303	5448	0.84	-	-	98.3
$5.0x10^{-5}$	1.0	536	2079	0.83	-	-	99.1
$1.0x10^{-4}$	1.1	695	995	0.81	-	-	99.3
$5.0x10^{-4}$	1.2	725	506	0.81	-	-	99.3
$1.0x10^{-3}$	1.1	798	171	0.79	-	-	99.4
72 h							
Blank	1.2	4	19642	0.90	0.4	0.4	-
$1.0x10^{-5}$	1.2	247	9792	0.82	-	-	98.4
$5.0x10^{-5}$	1.1	525	4024	0.81	-	-	99.2
$1.0x10^{-4}$	1.3	656	2028	0.79	-	-	99.4
$5.0x10^{-4}$	1.2	720	1325	0.79	-	-	99.4
$1.0x10^{-3}$	1.3	770	365	0.78	-	-	99.5
96 h							
Blank	1.3	4	38697	0.83	0.9	0.3	-
$1.0x10^{-5}$	1.1	174	20064	0.78	-	-	97.7
$5.0x10^{-5}$	1.2	374	9956	0.78	-	-	98.9
$1.0x10^{-4}$	1.0	488	3500	0.78	-	-	99.2
$5.0x10^{-4}$	1.0	610	1603	0.78	-	-	99.3
$1.0x10^{-3}$	1.0	630	549	0.77	-	-	99.4
120 h							
Blank	1.4	4	36520	0.89	0.4	0.3	-
$1.0x10^{-5}$	1.0	134	20108	0.77	-	-	97.0
$5.0x10^{-5}$	1.3	278	10002	0.75	-	-	98.6
$1.0x10^{-4}$	1.2	402	3750	0.75	-	-	99.0
$5.0x10^{-4}$	1.1	490	1803	0.74	-	-	99.2
$1.0x10^{-3}$	1.1	525	672	0.60	-	-	99.2

corrosion process of the mild steel is mostly carried out by the charge transfer [32, 33]. When interpreting the polarization resistance in EIS experiments, it would be more accurate to define it, considering its total charge transfer and diffusive layer resistance. In all impedance plots, the diameter of the capacitive loop boosted due to the increment of inhibitor concentration for each immersion time in the high frequency region.

In other words, the higher the inhibitor concentration, the greater the polarization resistance and inhibitory efficiency values (Table 2). Similar results in the literature have been reported in some researches [34–36]. When the

diagrams in the solutions with FG-FCF are examined, depressed loops are seen in both frequency regions. The loop in the low frequency region defines the film resistance and other accumulated types like corrosion products, while charge transfer and diffuse layer resistances are responsible for the high frequency region. This finding has been harmonious with many investigations in literature [37–39].

R_s values, according to Table 2, were generally constant for all concentrations and immersion times of about 1 Ω. The highest value of polarization resistance and thus the value of inhibition efficiency were calculated with $1.0\text{x}10^{-3}$ M FG-FCF solution at the end of the 1 h immersion time and values are 935 Ω and 92.3%, respectively. This high result is a clear indication of the extent to which it protects the metal surface at the end of 1 h immersion. As can be explicitly seen from Figures 3 and 4 and Table 2, the diameters of the curves, as a result of the expected corrosion process, have decreased with the boosting in immersion time.

The value of η% used in Table 2 was calculated using the equation given below:

$$\eta\,(\%) = \left(\frac{R'_p - R_p}{R'_p}\right) \times 100 \quad (1)$$

where R'_p and R_p are inhibited and uninhibited polarization resistance values, respectively.

The decrease in CPE values at all concentrations as the R_p values boost, it can be clearly clarified by the increment in the double layer thickness between the metal and the inhibitor or the reduction in the local dielectric constant [40]. The "n" value found by fitting the curves via the Zview2 program is the surface inhomogeneity coefficient of the metal. These values diminished at the end of each immersion period with the boost in inhibitor concentration. On account of boosting the FG-FCF concentration and decreasing the "n" values can be suggested as a proof of the adsorption of more FG-FCF molecules on the mild steel by reducing the active surface area. The EIS plots in Figures 3 and 4 are semielliptical as seemed.

In Table 2, the resistance range of R_p in inhibited solutions after 1 h was 576–935 Ω, 520–864 Ω after 24 h, 303–798 Ω after 48 h, 247–770 Ω after 72 h, 174–630 Ω after 96 h, and 134–525 Ω after 120 h. As the immersion time increased, there was still a significant inhibition in the η% values even though the R_p values decreased at each concentration. For instance, the η% values calculated from 1, 24, 48, 72, 96, and 120 h immersion times with the optimum concentration of FG-FCF are, respectively, 92.3%, 98.7, 99.4, 99.5, 99.4, and 99.2. This result reveals that the preventative and tight film grows well together with the rise of concentration of inhibitor and covers the surface just like a blanket. Figure 5 graphically depicts the distribution of the inhibition efficiency values together with the immersion times and concentration.

Figure 5 clearly indicates that FG-FCF has a very high protective influence. According to this graph and Table 2, the inhibitor efficiency values enhanced outstandingly up to 72 h and remained constant at about 99% at 96 and 120 h with a very slight diminish. The reason for this high protection effect is that five aromatic rings in the molecular structure of

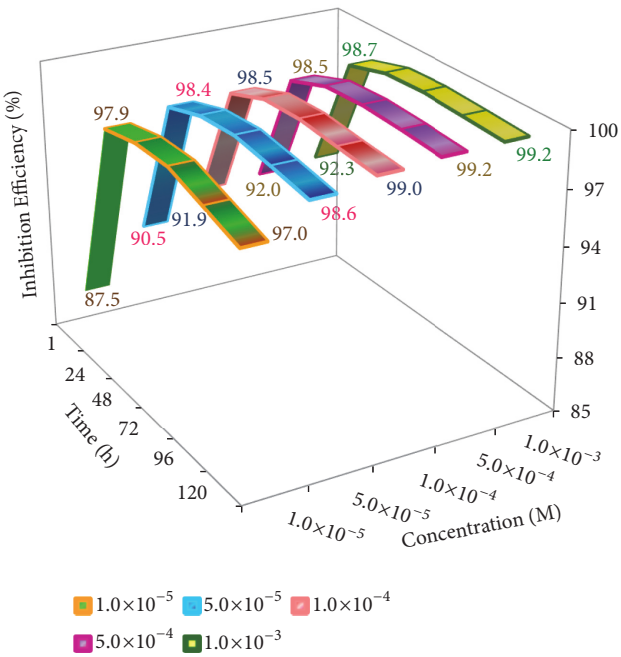

Figure 5: The distribution graph of the values of the inhibition efficiency together with the immersion time and concentration.

the FG-FCF inhibitor and the electron-donating π-electrons in these rings, as well as heteroatoms such as substituted nitrogen, sulphur, and oxygen, and the unpaired electrons found in these heteroatoms, by activating the inhibitor sufficiently, the metal surface is almost fully covered.

The potential of zero charge is another important variable depending on the adsorption concept. The adsorption activity of the inhibitors is influenced by the structure of the metal, the surface charge, and the molecular structure of the inhibitors. The surface charge of the metal is due to the electrical field between the metal and the inhibitor. For this reason, EIS method was used to determine the zero charge potential of mild steel. When determining the surface charge of metal, R_p values were plotted against E_{corr} values and Figure 6 was formed. The maximum peak in this graph is E_{pzc}. The charge of metal was determined by comparing the position of corrosion potential with E_{pzc}. Equation related to this is as follows:

$$\Psi = E_{corr} - E_{pzc} \quad (2)$$

where E_{corr} is the corrosion potential, E_{pzc} is the zero charge potential, and Ψ is the surface charge of mild steel.

The surface charge may be in two ways, either positive or negative. If the surface charge is determined to be positive, there is the adsorption of anions to the surface. If negative, the cations will first want to adsorb to the surface [41]. E_{pzc} of the mild steel was studied in 1.0 M HCl with $1.0\text{x}10^{-3}$ M FG-FCF solution. The all tested R_p values were recorded at a stable potential within ± 0.250 V (Ag/AgCl).

According to Figure 6, the potential difference between E_{corr} and E_{pzc} is Ψ = -0.05 V. In this case, the negative presence of Ψ indicates that the metal surface is negatively charged.

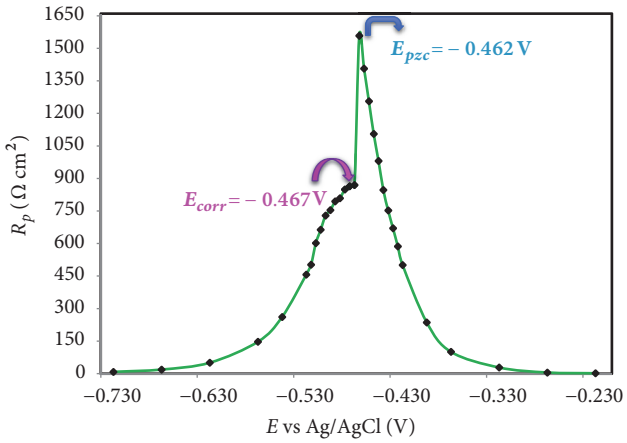

Figure 6: Plot of R_p versus applied electrode potential of mild steel in 1.0 M HCl with 1.0x10^{-3} M FG-FCF.

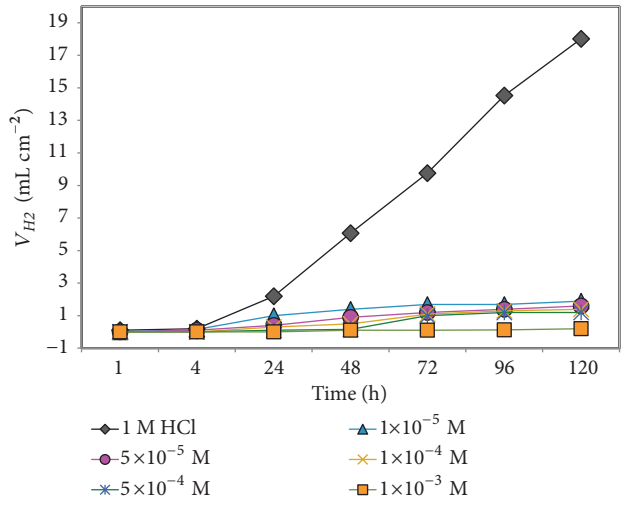

Figure 7: Hydrogen volume amount evolved of mild steel immersed in 1.0 M HCl at different concentrations of FG-FCF.

Thus, it can be said that the protonated water molecules and cationic species of the inhibitor are adsorbed directly to the metal surface [42]. At the same time, material loss is reduced.

3.2. Hydrogen Evolution Tests. The corrosion of mild steel in 1.0 M HCl with the nonexistence and existence of inhibitor as a function of time at 298 K by applying gasometry method are plotted in Figure 7.

With this method, it is possible to calculate η% versus immersion time from the hydrogen gas volume by means of the following equation [43].

$$\eta\,(\%) = \left(\frac{V - V'}{V}\right) \times 100 \tag{3}$$

where V and V' are the hydrogen gas volumes in the nonexistence and existence of inhibitor, respectively. As is evident from Figure 7, there is a clear difference between the blank solution and the five concentrations of the inhibitor.

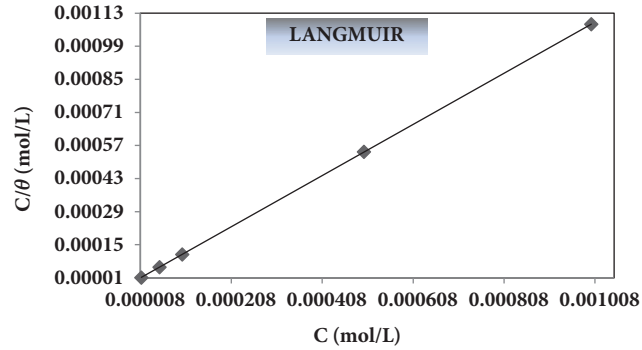

Figure 8: Langmuir adsorption plot for mild steel in 1.0 M HCl solution containing five concentrations of FG-FCF inhibitor.

As the concentration of the inhibitor increases, the volume of hydrogen gas exiting the electrode surface decreases even if the immersion time of the electrode increases. So again, there is significant inhibition performance for the dissolution process. With this method, the maximum inhibition activity calculated in the 1.0x10^{-3} M FG-FCF solution at the end of the longest immersion time (120 h) was 98.9%, while these values were gradually 93.4%, 92.3%, 91.2%, and 89.5% for the concentration of 5.0x10^{-4}M, 1.0x10^{-4}M, 5.0x10^{-5}M, and 1.0x10^{-5} M, respectively. Even at the end of the 120 h, there is still an influential protection of over 90%. In other words, as the FG-FCF is added to the acidic medium, the hydrogen gas evolution is substantially declined. This implies that the FG-FCF molecules are adsorbed tightly to the surface of mild steel and inhibited by reducing the active surface [44]. The findings acquired from this method were consistent with EIS findings.

3.3. Determination of Adsorption Isotherm. The inhibitor can inhibit the metal corrosion in two ways. In the first, inhibitor molecules can be adsorbed directly onto the metal surface or else, there may be interactions between the charged metal surface and the charged molecule. This step of the study draws attention to the understanding of the mechanism of inhibition, that is, how the FG-FCF inhibitor interacts with the mild steel surface. In other words, it leads to the understanding that FG-FCF is adsorbed to the mild steel surface by chemical adsorption or physical adsorption. In order to understand the mechanism of inhibition of FG-FCF, the θ (surface coverage coefficient) values obtained due to the immersion time (1-120 h) in EIS are plotted. Five different adsorption isotherms such as Langmuir, Florry-Huggins, Temkin, Frumkin, and Freundlich have been tried. Among these plots, the highest R^2 (correlation coefficient) value was obtained by Langmuir adsorption isotherm. The corresponding equation of the Langmuir adsorption isotherm is as follows:

$$\frac{C_{(inh)}}{\theta} = \frac{1}{K_{(ads)}} + C \tag{4}$$

where $C_{(inh)}$ is the FG-FCF concentration and $K_{(ads)}$ is the adsorption equilibrium constant of the adsorption process. C versus C/θ plot grants a linear line with a slope near unit

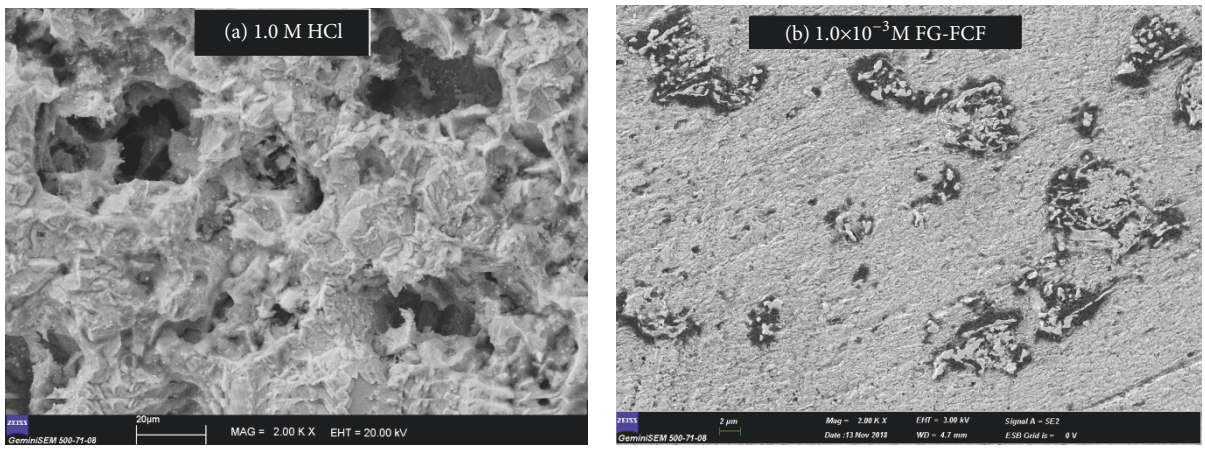

(a) (b)

Figure 9: FESEM images of 1.0 M HCl and 1.0x10^{-3} M FG-FCF in 1.0 M HCl solution after 120 h.

Table 3: The K_{ads} and ΔG°_{ads} values of FG-FCF found from Langmuir isotherm for each immersion times.

Immersion time (h)	K_{ads}	ΔG°_{ads} (kJ/mol)
1	1111111.11	-44.44
24	3333333.33	-47.16
48	5000000.00	-48.17
72	5000000.00	-48.17
96	3333333.33	-47.16
120	5000000.00	-48.17

(Figure 8). Figure 8 reveals only the graph of the immersion time of 1 h in a representative manner.

From the Langmuir isotherms plotted for each immersion time, the adsorption-free energy (ΔG°_{ads}) and the adsorption equilibrium constant (K_{ads}) values mentioned in Table 3 were calculated by means of

$$K_{ads} = \frac{1}{55.5}\exp\left(-\frac{\Delta G^{\circ}_{ads}}{RT}\right) \quad (5)$$

where 55.5 is the molar concentration of water, R is the universal gas constant, and T is temperature in Kelvin.

Literature researches uncover that the values of ΔG°_{ads} around -20 kJ/mol or less negative than are convenient with the electrostatic interaction between the charged inhibitor molecules and the charged metal surface (physisorption) and those around -40 kJ/mol or more negative (Table 3) than included sharing or charge transfer of electrons between inhibitor molecules and the surface of mild steel to constitute bond of a coordinate type (chemisorption) [45, 46]. In this study, all ΔG°_{ads} values calculated (Table 3) for each immersion times are largely more negative than -40 kJ/mol and incorporate chemisorption, charge sharing between inhibitor, and metal surface. This signify that the unshared electron pairs of nitrogen, oxygen, and sulphur atoms situated in FG-FCF molecular structure could interact with d-orbitals of Fe atom to form a preventive chemisorbed film. Furthermore, the chemical structure of FG-FCF increases the chemical adsorption ability onto the metal to form a coordinated bond between the unpaired electrons of heteroatoms in the structure, the π-electrons in the aromatic rings, and the mild steel surface. The negative magnitude of ΔG°_{ads} is a determinant of the thermodynamic spontaneously of the adsorption process.

3.4. Surface Characteristics. Surface characteristics were analysed by FESEM and AFM methods in order to interpret the surface images of the mild steel specimens in 1.0 M HCl solution at the end of 120 h immersion time for 298 K. FESEM and AFM images were performed in 1.0 M HCl solutions with and without 1.0x10^{-3} M. These analyses were conducted by cutting the mild steel specimens at a distance of 0.5 cm from the surface with the iron saw. FESEM micrographs of the specimens for the FG-FCF inhibitor magnified 2000-fold are presented in Figure 9. FESEM has higher resolution and a much greater energy range than SEM.

It can readily be monitored from Figure 9(a) that huge dark spots are seen in the pit-like appearance on the specimen surface immersed in the blank solution. Thus, it can be explicitly called that this specimen is noticeably oxidized and distorted by the blank solution. In contrast to the blank solution, the surface in the FG-FCF medium is almost completely covered with the inhibitor and appears to be smoother and cleaner surface (Figure 9(b)) [47, 48].

AFM is a sophisticated and advantageous technique for analysing at the nanoscale. The images can be obtained at the molecular level or can be taken directly from the surfaces. It can provide important information about surface properties, morphologies, and roughness [49]. The 3D-AFM images of specimens subjected to in 1.0 M HCl with and without 1.0x10^{-3} M FG-FCF for 120 h are given in Figures 10(a) and 10(b), respectively.

The consequences of AFM images are very harmonious with those of FESEM. As can be seen from Figure 10(a), the mild steel specimen is exceedingly impressed by the aggressive solution and turned into a rough and porous surface with

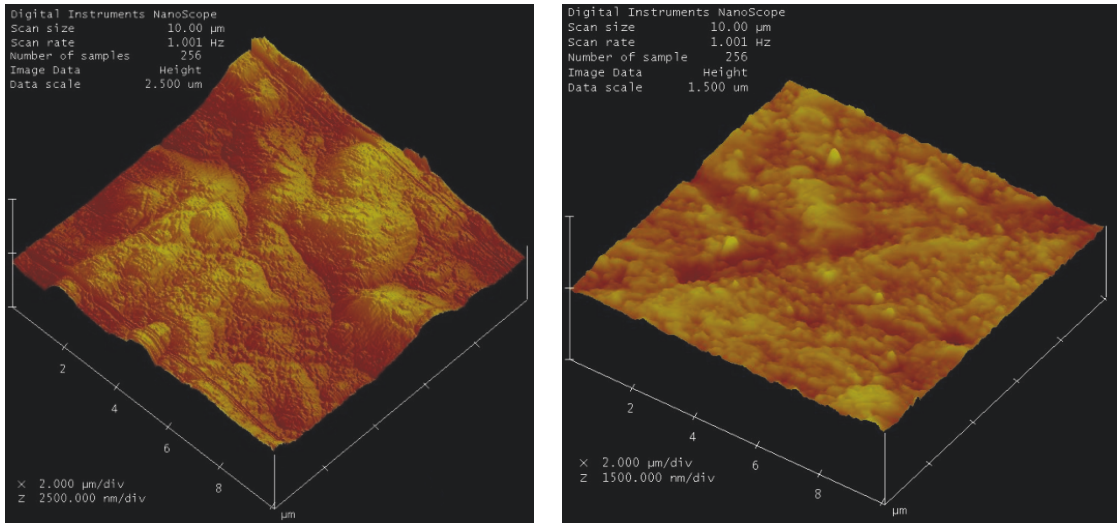

(a) 1.0 M HCl (b) $1.0x10^{-3}$ M FG-FCF

Figure 10: AFM images of 1.0 M HCl and $1.0x10^{-3}$ M FG-FCF in 1.0 M HCl solution after 120 h.

large and deep pits. The average roughness of the surface was determined to be 197.66 nm. This value was determined as 29.54 nm by adding $1.0x10^{-3}$ M FG-FCF to the acidic medium (Figure 10(b)). It has also been affirmed by AFM method that the electrode surface, which are containing the FG-FCF solution for 120 h, has a proper and fairly cleaner structure. When the average surface roughness values are taken into account, it is recorded that the value in FG-FCF solution is significantly less than the value in the blank solution. As a result, it can be said that surface characterization studies are another proof that the inhibitor examined considerably inhibits the corrosion of mild steel.

4. Conclusions

In this study, the usage of Fast Green-FCF as a corrosion inhibitor in addition to its use in food dye and protein staining was examined in 1.0 M HCl for different immersion times by using electrochemical measurement methods. The following results can be underlined:

(1) At the end of this study, it was concluded that FG-FCF is an excellent inhibitor that can be used in practice in order to prevent the long-term corrosion of mild steel in 1.0 M HCl medium.

(2) Its inhibition efficiency is not only dependent on the concentration but also on the long-term. The excellent inhibition of FG-FCF is due to its tight covering of the mild steel surface just like a blanket.

(3) In the hydrogen evolution experiments, the minimum gas volume change was observed at optimum concentration.

(4) It can be highlighted that the surface of the mild steel is negatively charged and that the protonated FG-FCF molecules are adsorbed directly onto the metal surface.

(5) The adsorption of FG-FCF on the surface of mild steel follows the Langmuir isotherm. The negative values of ΔG°_{ads} point out that inhibitor molecule were strongly and spontaneously chemisorbed onto the mild steel surface.

(6) FESEM and AFM images explicitly reveal that deep pits were closed with addition of FG-FCF to acidic medium and it is increasingly got smoother and cleaner surface.

Data Availability

The data used to support the findings of this study are included within the article.

Conflicts of Interest

The author declares that there are no conflicts of interest regarding the publication of this manuscript.

References

[1] https://sciencing.com/mechanical-properties-mild-steel-6618717.html.

[2] R. A. Prabhu, T. V. Venkatesha, A. V. Shanbhag, G. M. Kulkarni, and R. G. Kalkhambkar, "Inhibition effects of some Schiff's bases on the corrosion of mild steel in hydrochloric acid solution," *Corrosion Science*, vol. 50, no. 12, pp. 3356–3362, 2008.

[3] H. Keleş and M. Keleş, "Protection effect of 2-(phenylthio)phenyl)-1-(2-(trifluoromethyl)phenyl) methanimine on Low carbon steel at open circuit and different potentials," *Protection of Metals and Physical Chemistry of Surfaces*, vol. 54, no. 3, pp. 513–525, 2018.

[4] V. S. Sastri, in *Green Corrosion Inhibitors: Theory and Practice*, pp. 257–303, John Wiley & Sons, Inc., Hoboken, New Jersey, USA, 2011.

[5] Y. I. Kuznetsov, A. D. Mercer, and J. G. Thomas, in *Organic Corrosion Inhibitors for Cooling Systems*, pp. 225–246, Springer Science+Business Media, Plenum Press, New York, USA, 1996.

[6] R. Yıldız, "Adsorption and inhibition effect of 2,4-diamino-6-hydroxypyrimidine for mild steel corrosion in HCl medium: experimental and theoretical investigation," *Ionics*, vol. 24, pp. 1–12, 2018.

[7] K. Shanmuga priya, B. Prathibha, V. Vasudha, and H. Nagaswarupa, "Spathodea campanulata as a corrosion inhibitor for mild steel in 1N H2SO4 media," *Materials Today: Proceedings*, vol. 5, no. 10, pp. 22595–22604, 2018.

[8] Q. Zhang, B. Hou, N. Xu, H. Liu, and G. Zhang, "Two novel thiadiazole derivatives as highly efficient inhibitors for the corrosion of mild steel in the CO2-saturated oilfield produced water," *Journal of the Taiwan Institute of Chemical Engineers*, 2018.

[9] C. Verma, E. E. Ebenso, and M. A. Quraishi, "Ionic liquids as green and sustainable corrosion inhibitors for metals and alloys: An overview," *Journal of Molecular Liquids*, vol. 233, pp. 403–414, 2017.

[10] E. Li, J. Wu, D. Zhang, Y. Sun, and J. Chen, "D-phenylalanine inhibits the corrosion of Q235 carbon steel caused by Desulfovibrio sp.," *International Biodeterioration & Biodegradation*, vol. 127, pp. 178–184, 2018.

[11] A. El Nemr, A. A. Moneer, A. Khaled, A. El Sikaily, and G. F. El-Said, "Modeling of synergistic halide additives' effect on the corrosion of aluminum in basic solution containing dye," *Materials Chemistry and Physics*, vol. 144, no. 1-2, pp. 139–154, 2014.

[12] R. Jia, T. Unsal, D. Xu, Y. Lekbach, and T. Gu, "Microbiologically influenced corrosion and current mitigation strategies: A state of the art review," *International Biodeterioration & Biodegradation*, vol. 137, pp. 42–58.

[13] A. Singh, Y. Lin, W. Liu et al., "Plant derived cationic dye as an effective corrosion inhibitor for 7075 aluminum alloy in 3.5% NaCl solution," *Journal of Industrial and Engineering Chemistry*, vol. 20, no. 6, pp. 4276–4285, 2014.

[14] E. Pensini, R. van Lier, F. Cuoq, W. Hater, and T. Halthur, "Enhanced corrosion resistance of metal surfaces by film forming amines: A comparative study between cyclohexanamine and 2-(diethylamino)ethanolbased formulations," *Water Resources and Industry*, vol. 20, pp. 93–106, 2018.

[15] M. Abd El-raouf, O. E. El-Azabawy, and R. E. El-Azabawy, "Investigation of adsorption and inhibitive effect of acid red GRE (183) dye on the corrosion of carbon steel in hydrochloric acid media," *Egyptian Journal of Petroleum*, vol. 24, no. 3, pp. 233–239, 2015.

[16] I. M. Baghni, S. B. Lyon, and B. Ding, "The effect of strontium and chromate ions on the inhibition of zinc," *Surface and Coatings Technology*, vol. 185, no. 2-3, pp. 194–198, 2004.

[17] Y. Abboud, A. Abourriche, T. Saffaj et al., "A novel azo dye, 8-quinolinol-5-azoantipyrine as corrosion inhibitor for mild steel in acidic media," *Desalination*, vol. 237, no. 1-3, pp. 175–189, 2009.

[18] S. Pareek, D. Jain, S. Hussain et al., "A new insight into corrosion inhibition mechanism of copper in aerated 3.5 wt.% NaCl solution by eco-friendly Imidazopyrimidine Dye: experimental and theoretical approach," *Chemical Engineering Journal*, vol. 358, pp. 725–742, 2019.

[19] E. E. Ebenso and E. E. Oguzie, "Corrosion inhibition of mild steel in acidic media by some organic dyes," *Materials Letters*, vol. 59, no. 17, pp. 2163–2165, 2005.

[20] C. Lei, X. Zhu, B. Zhu, C. Jiang, Y. Le, and J. Yu, "Superb adsorption capacity of hierarchical calcined Ni/Mg/Al layered double hydroxides for Congo red and Cr(VI) ions," *Journal of Hazardous Materials*, vol. 321, pp. 801–811, 2017.

[21] D. S. Moreno, H. Celedonio, R. L. Mangan, J. L. Zavala, and P. Montoya, "Field evaluation of a phototoxic dye, phloxine B, against three species of fruit flies (Diptera: Tephritidae)," *Journal of Economic Entomology*, vol. 94, no. 6, pp. 1419–1427, 2001.

[22] T. I. Tikhomirova, G. R. Ramazanova, and V. V. Apyari, "Effect of nature and structure of synthetic anionic food dyes on their sorption onto different sorbents: Peculiarities and prospects," *Microchemical Journal*, vol. 143, pp. 305–311, 2018.

[23] N. P. Shetti, D. S. Nayak, and S. J. Malode, "Electrochemical behavior of azo food dye at nanoclay modified carbon electrode-a nanomolar determination," *Vacuum*, vol. 155, pp. 524–530, 2018.

[24] E. Guerra, G. Alvarez-Rivera, M. Llompart, and C. Garcia-Jares, "Simultaneous determination of preservatives and synthetic dyes in cosmetics by single-step vortex extraction and clean-up followed by liquid chromatography coupled to tandem mass spectrometry," *Talanta*, vol. 188, pp. 251–258, 2018.

[25] S. Tsuji, K. Yoshii, and Y. Tonogai, "Identification of isomers and subsidiary colors in commercial Fast Green FCF (FD&C Green No. 3, Food Green No. 3) by liquid chromatography-mass spectrometry and comparison between amounts of the subsidiary colors by high-performance liquid chromatography and thin-layer chromatography- spectrophotometry," *Journal of Chromatography A*, vol. 1101, no. 1-2, pp. 214–221, 2006.

[26] J. A. Van Hooft, "Fast Green FCF (Food Green 3) inhibits synaptic activity in rat hippocampal interneurons," *Neuroscience Letters*, vol. 318, no. 3, pp. 163–165, 2002.

[27] J. Pooralhossini, M. Ghaedi, M. A. Zanjanchi, and A. Asfaram, "Ultrasonically assisted removal of Congo Red, Phloxine B and Fast green FCF in ternary mixture using novel nanocomposite following their simultaneous analysis by derivative spectrophotometry," *Ultrasonics Sonochemistry*, vol. 37, pp. 452–463, 2017.

[28] A. Mittal, D. Kaur, and J. Mittal, "Batch and bulk removal of a triarylmethane dye, Fast Green FCF, from wastewater by adsorption over waste materials," *Journal of Hazardous Materials*, vol. 163, no. 2-3, pp. 568–577, 2009.

[29] P. Koli, "Solar energy conversion and storage: Fast Green FCF-Fructose photogalvanic cell," *Applied Energy*, vol. 118, pp. 231–237, 2014.

[30] A. Fitoz, H. Nazır, M. Özgür (nee Yakut), E. Emregül, and K. C. Emregül, "An experimental and theoretical approach towards understanding the inhibitive behavior of a nitrile substituted coumarin compound as an effective acidic media inhibitor," *Corrosion Science*, vol. 133, pp. 451–464, 2018.

[31] D. Özkir, K. Kayakirilmaz, E. Bayol, A. A. Gürten, and F. Kandemirli, "The inhibition effect of Azure A on mild steel in 1M HCl. A complete study: adsorption, temperature, duration and quantum chemical aspects," *Corrosion Science*, vol. 56, pp. 143–152, 2012.

[32] R. Solmaz, "Investigation of adsorption and corrosion inhibition of mild steel in hydrochloric acid solution by 5-(4-Dimethylaminobenzylidene)rhodanine," *Corrosion Science*, vol. 79, pp. 169–176, 2014.

[33] D. Özkir and E. Bayol, "Inhibition efficiency of benzidine for mild steel in acidic media," *Protection of Metals and Physical Chemistry of Surfaces*, vol. 47, no. 4, pp. 517–527, 2011.

[34] T. N. J. I. Edison, R. Atchudan, A. Pugazhendhi, Y. R. Lee, and M. G. Sethuraman, "Corrosion inhibition performance of

spermidine on mild steel in acid media," *Journal of Molecular Liquids*, vol. 264, pp. 483–489, 2018.

[35] B. Dogru Mert, M. E. Mert, G. Kardas, and B. Yazici, "The experimental and quantum chemical investigation for two isomeric compounds as aminopyrazine and 2-amino-pyrimidine against mild steel corrosion," *Anti-Corrosion Methods and Materials*, vol. 63, no. 5, pp. 369–376, 2016.

[36] M. Faustin, A. Maciuk, P. Salvin, C. Roos, and M. Lebrini, "Corrosion inhibition of C38 steel by alkaloids extract of Geissospermum laeve in 1M hydrochloric acid: Electrochemical and phytochemical studies," *Corrosion Science*, vol. 92, pp. 287–300, 2015.

[37] M. Prajila and A. Joseph, "Inhibition of mild steel corrosion in hydrochloric using three different 1,2,4-triazole Schiff's bases: A comparative study of electrochemical, theoretical and spectroscopic results," *Journal of Molecular Liquids*, vol. 241, pp. 1–8, 2017.

[38] A. Döner, E. A. Şahin, G. Kardaş, and O. Serindağ, "Investigation of corrosion inhibition effect of 3-[(2-hydroxy-benzylidene)-amino]-2-thioxo-thiazolidin-4-one on corrosion of mild steel in the acidic medium," *Corrosion Science*, vol. 66, pp. 278–284, 2013.

[39] D. Özkir, "Yumuşak çeliğin korozyon inhibitörlerine kloroanilinden sentezlenen yeni bir örnek: 2-[(2,5-diklorofenilimino)metil]fenol," *Ömer Halisdemir Üniversitesi Mühendislik Bilimleri Dergisi*, vol. 7, no. 2, pp. 993–1003, 2018.

[40] A. Espinoza-Vázquez, G. E. Negrón-Silva, R. González-Olvera et al., "Mild steel corrosion inhibition in HCl by di-alkyl and di-1,2,3-triazole derivatives of uracil and thymine," *Materials Chemistry and Physics*, vol. 145, no. 3, pp. 407–417, 2014.

[41] H. M. Abd El-Lateef, A. M. Abu-Dief, L. H. Abdel-Rahman, E. C. Sañudo, and N. Aliaga-Alcalde, "Electrochemical and theoretical quantum approaches on the inhibition of C1018 carbon steel corrosion in acidic medium containing chloride using some newly synthesized phenolic Schiff bases compounds," *Journal of Electroanalytical Chemistry*, vol. 743, pp. 120–133, 2015.

[42] C. B P and P. Rao, "Environmentally benign green inhibitor to attenuate acid corrosion of 6061Aluminum-15%(v) SiC(P) composite," *Journal of Industrial and Engineering Chemistry*, vol. 58, pp. 357–368, 2018.

[43] A. A. El-Meligi, "Hydrogen production by aluminum corrosion in hydrochloric acid and using inhibitors to control hydrogen evolution," *International Journal of Hydrogen Energy*, vol. 36, no. 17, pp. 10600–10607, 2011.

[44] E. S. El Tamany, S. Elsaeed, H. Ashour, E. Zaki, and H. El Nagy, "Novel acrylamide ionic liquids as anti-corrosion for X-65 steel dissolution in acid medium: Adsorption, hydrogen evolution and mechanism," *Journal of Molecular Structure*, vol. 1168, pp. 106–114, 2018.

[45] P. Arellanes-Lozada, O. Olivares-Xometl, N. V. Likhanova, I. V. Lijanova, J. R. Vargas-García, and R. E. Hernández-Ramírez, "Adsorption and performance of ammonium-based ionic liquids as corrosion inhibitors of steel," *Journal of Molecular Liquids*, vol. 265, pp. 151–163, 2018.

[46] S. A. Umoren, A. A. AlAhmary, Z. M. Gasem, and M. M. Solomon, "Evaluation of chitosan and carboxymethyl cellulose as ecofriendly corrosion inhibitors for steel," *International Journal of Biological Macromolecules*, vol. 117, pp. 1017–1028, 2018.

[47] M. Moradi, Z. Song, T. Xiao et al., "Exopolysaccharide produced by Vibrio neocaledonicus sp. as a green corrosion inhibitor: Production and structural characterization," *Journal of Materials Science and Technology*, vol. 34, no. 12, pp. 2447–2457, 2018.

[48] M. Murmu, S. K. Saha, N. C. Murmu, and P. Banerjee, "Effect of stereochemical conformation into the corrosion inhibitive behaviour of double azomethine based Schiff bases on mild steel surface in 1 mol L^{-1} HCl medium: An experimental, density functional theory and molecular dynamics simulation study," *Corrosion Science*, vol. 146, pp. 134–151, 2019.

[49] I. Abdulazeez, A. Zeino, C. W. Kee et al., "Mechanistic studies of the influence of halogen substituents on the corrosion inhibitive efficiency of selected imidazole molecules: A synergistic computational and experimental approach," *Applied Surface Science*, vol. 471, pp. 494–505, 2019.